NANO LETTERS

2005
Vol. 5, No. 10
1931−1936

# Patterned Assembly of Genetically Modified Viral Nanotemplates via Nucleic Acid Hybridization

**Hyunmin Yi,[†] Saira Nisar,[‡] Sang-Yup Lee,[§] Michael A. Powers,[||] William E. Bentley,[‡,⊥] Gregory F. Payne,[‡] Reza Ghodssi,[||,#] Gary W. Rubloff,[†,#] Michael T. Harris,[§] and James N. Culver*[,‡]**

*Department of Materials Science and Engineering, University of Maryland, College Park, Maryland 20742, Center for Biosystems Research, University of Maryland Biotechnology Institute, College Park, Maryland 20742, School of Chemical Engineering, Purdue University, West Lafayette, Indiana 47907, Department of Electrical and Computer Engineering, University of Maryland, College Park, Maryland 20742, Department of Chemical and Biomolecular Engineering, University of Maryland, College Park, Maryland 20742, and Institute for Systems Research, University of Maryland, College Park, Maryland 20742*

*Received June 30, 2005; Revised Manuscript Received August 22, 2005*

**ABSTRACT**

**The patterning of nanoparticles represents a significant obstacle in the assembly of nanoscale materials and devices. In this report, cysteine residues were genetically engineered onto the virion surface of tobacco mosaic virus (TMV), providing attachment sites for fluorescent markers. To pattern these viruses, labeled virions were partially disassembled to expose 5′ end RNA sequences and hybridized to virus-specific probe DNA linked to electrodeposited chitosan. Electron microscopy and RNAase treatments confirmed the patterned assembly of the virus templates onto the chitosan surface. These findings demonstrate that TMV nanotemplates can be dimensionally assembled via nucleic acid hybridization.**

Biologically derived materials are increasingly being utilized to impart novel functionalities at the micro- and nanoscale level. For example, the integration of biological sensing components with microfabrication technologies has revolutionized methodologies for genomics, proteomics, and drug discovery. Biological components are also assuming a more direct role in the fabrication of nanoscale materials. DNA has been exploited as a template for the construction of metal-coated nanowires and used in combination with carbon nanotubes to create field effect transistors.[1,2] In addition, the genetically derived nanostructures of viruses have been exploited as templates for the creation of metallic and semiconductor nanospheres and wires.[3,4] Clearly, the extraordinary specificities and self-assembly properties of bioderived materials offer distinct advantages in the fabrication of new materials.

Filamentous plant viruses represent simple macromolecular assemblies, consisting of a single molecule of nucleic acid packaged by many copies of an identical coat protein. One of the best-studied filamentous viruses is tobacco mosaic virus (TMV). The TMV virion is a rigid rod consisting of ∼2130 identical coat protein subunits (MW 17.5 kDa)[5] stacked in a helix around a single strand of plus sense RNA, leaving a 4 nm diameter channel through an 18 × 300 nm rodlike virion (Figure 1).

The known structure and assembly intermediates of TMV as well as the ability to reverse engineer this virus make it a particularly versatile biotemplate for the production of nanoparticles.[5,6] Repeating arrangements of charged amino acids along the surface of the TMV virion can function in the nucleation of inorganic precursors, facilitating the mineralization of the virus.[7] Using the wild-type virus, nanoparticles consisting of silica, lead, platinum, gold, silver, iron oxides, and cadmium sulfides have been prepared on and within the rodlike virus particles of TMV using various reduction schemes.[8−11] In addition, diazonium and carbodi-

* Corresponding author: James N. Culver, Center for Biosystems Research, University of Maryland Biotechnology Institute, College Park, MD 20742. Ph: (301) 405-2912. Fax: (301) 314-9075. E-mail: jculver@umd.edu.

[†] Department of Materials Science and Engineering, University of Maryland.

[‡] Center for Biosystems Research, University of Maryland Biotechnology Institute.

[§] School of Chemical Engineering, Purdue University.

[||] Department of Electrical and Computer Engineering, University of Maryland.

[⊥] Department of Chemical and Biomolecular Engineering, University of Maryland.

[#] Institute for Systems Research, University of Maryland.

10.1021/nl051254r CCC: $30.25 
**Published on Web 09/02/2005**

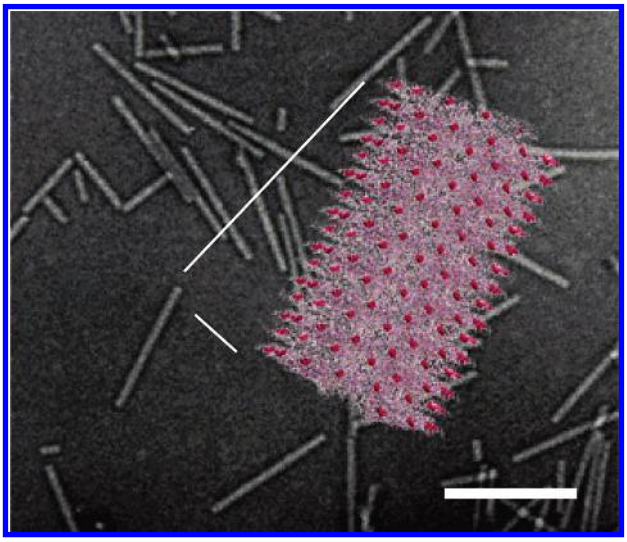

**Figure 1.** Visualization of TMV1cys. Background, electron micrograph of TMV (negatively stained). Bar represents 300 nm. Foreground, structural model representing ~10% of a TMV1cys virion. Red space filling molecules show the location of the genetically inserted cysteine residue.

imide coupling reactions have also been used to modify specific surface-charged TMV amino acids.[12]

Reverse genetic approaches have also been used to engineer viral templates with novel inorganic binding traits and mineralization properties.[13] For TMV, genetic alterations affecting the charge characteristics of the inner channel have been shown to alter the deposition of inorganic quantum dots.[7] Furthermore, thiol linkages conferred by the addition of multiple cysteine residues to the outer surface of TMV enhance the uniformity and binding strength of reaction precursors, significantly enhancing mineralization[14] (Supporting Information). Thus, TMV functions as a malleable biosubstrate for the template-assisted growth of nanoparticles.

Another unique feature of TMV is the polar nature of its virion. The helical encapsidation of the viral RNA results in sequence definable 5′ and 3′ ends within the rod-shaped virus particle. Each TMV coat protein is capable of interacting with three nucleotides of the viral RNA. In addition, coat protein−RNA interactions are strongest when a guanine residue occupies the third position of the binding site.[15] Interestingly, there are no guanine residues within the 5′ leader sequence or first 69 nucleotides of the viral RNA[16]. However, there is a clear bias for guanine in the third position throughout the rest of the viral genome.[17] Thus, coat protein−RNA interactions are weakest at the 5′ end of the viral RNA. Within a cell, exposure of the RNA 5′ end promotes ribosome binding and protein translation, resulting in the further disassembly of the virion via a process termed cotranslation disassembly.[18] Biologically this represents an elegant evolutionary adaptation that allows the viral RNA to remain encapsidated and protected from the cellular environment until active translation and replication is initiated. For the purposes of this study, mild alkaline treatments and centrifugation can be used to mimic cellular conditions so as to partially disassemble the virus and expose the 5′ end of its genome.[18] We hypothesized that exposed TMV RNA 5′ end sequences could function, via nucleic acid hybridization, to address virus nanotemplates in a spatially oriented manner.

Technologies for the construction and measurement of nanoscale objects are currently receiving a great deal of attention. However, there exist considerable obstacles to the patterning and assembly of nanomaterials into functional devices. At present nanocircuits are generally formed by flowing a liquid suspension of nanowires/particles over prefabricated electrodes. Nanowires that settle between desired electrodes can then be fabricated into usable devices. However, this process lacks specificity and uses only a fraction of the available nanoparticles. Alternative methods, such as microcontact printing and dip-pen nanolithography, can provide a direct "top-down" means for patterning materials at the nano and molecular level.[19] However, these approaches generally require complex surface chemistries and expensive robotic technologies.[20−22] Recently, the aminopolysaccharide chitosan has been utilized to link biological molecules to microfabricated surfaces in a spatially selective manner by electrodeposition.[23−25] Chitosan's primary amines function as a pH-dependent solubility switch, such that at low pH (<6.3) the amines are protonated and chitosan becomes water soluble, while at high pH the amines become deprotonated with chitosan losing its charge and becoming insoluble. The effects of pH on the solubility of chitosan allow it to be electrodeposited onto any cathode surface.[25] Chitosan's primary amines also provide a simple means for the covalent tethering of various biomolecules including proteins and nucleic acids. Thus, chitosan provides a unique interface between "top-down" microfabrication techniques and "bottom-up" bio-nanoassemblies.

We report here the creation and patterning of a new TMV-based nanoparticle template using nucleic acid hybridization (Figure 2). Specifically, we genetically engineered a cysteine residue onto the surface of the TMV coat protein to function in the attachment of thiol reactive fluorescent markers. Functionalized TMV particles were partially disassembled to expose the 5′ end of the viral genome and hybridized to complementary probe DNA linked to electropatterned chitosan-coated silicon chips. Results demonstrated that functionalized TMV templates could be specifically addressed as well as oriented using this hybridization-based assembly approach. Taken together these findings demonstrate the usefulness of an integrated approach that combines "top-down" silicon-based lithography with "bottom-up" biologically assembled nanoparticle templates for the fabrication of novel devices.

**Genetic Manipulation of the TMV Coat Protein.** A full-length infectious cDNA clone of the U1 strain of TMV, pSNC004, was used as the parental construct for the creation of TMV1cys.[6,26] The addition of a single cysteine residue within the TMV coat protein was created by the insertion of a TGT codon at the third position within the coat protein open reading frame using a PCR-based mutagenesis procedure.[27] Infectious RNA transcripts generated from the full-length TMV1cys construct were used to inoculate *Nicotiana tabacum*, cv Xanthi, a systemic TMV host. Inoculated plants

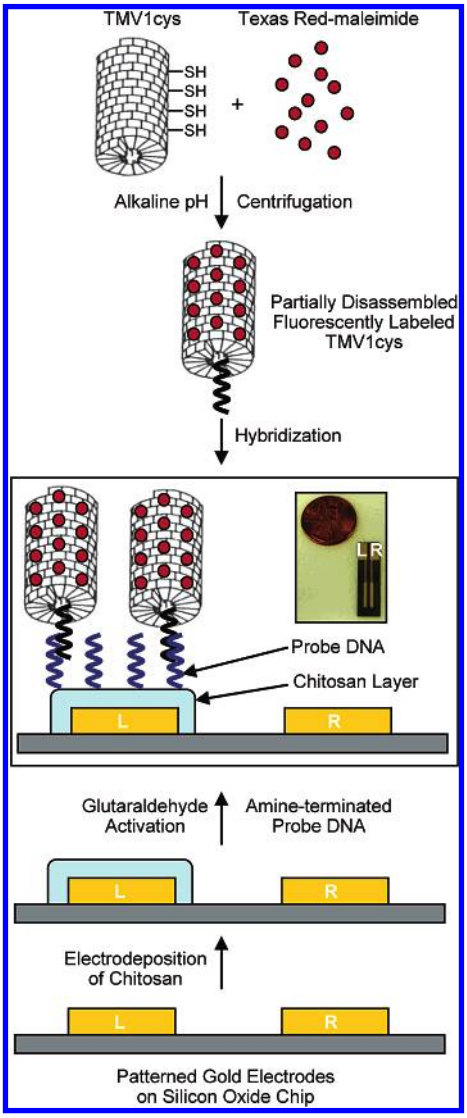


**Figure 2.** Diagram for the DNA probe directed assembly of TMV1cys nanotemplates onto a readily addressable site. L and R represent left and right electrodes. Inserted picture shows an actual chip.

were harvested at 20 days postinoculation and virus purified as previously described.[28] Reverse transcribed PCR followed by DNA sequencing was used to confirm the maintenance of the 1cys insertion in the coat protein ORFs of purified virus.

**Fluorescent Labeling of TMV1cys Virions.** For fluorescent labeling, purified TMV1cys (150 $\mu$g/mL) was incubated for 1 h in the presence of 5-fold molar excess of Texas Red or Rhodamine maleimide (Molecular Probes, Eugene OR) in 50 mM Tris buffer, pH 7.0. Labeled virus was separated by centrifugation in a 10−40% sucrose gradient at 45*g* for 2 h (Figure 3). Banded viruses were harvested via a syringe and pH adjusted to 8.0 to partially remove coat protein subunits from the 5′ ends of the viral genome. Partially disassembled virions were pelleted by centrifugation for 2 h at 65*g* to remove free coat proteins. Pelleted viruses (10 to 20 $\mu$g/mL) were resuspended in 2×SSC buffer (30 mM sodium citrate, 300 mM sodium chloride, pH 7.0) containing 5 mM DTT.

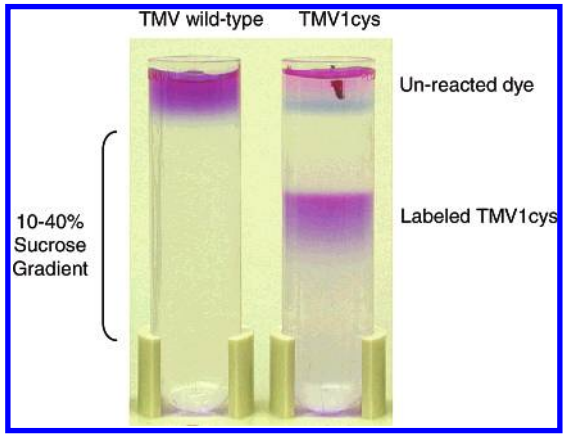


**Figure 3.** Specificity for the labeling of TMV1cys virions. 100 $\mu$g of purified TMV wild-type or TM1cys virus was incubated for 1 h in 5 molar excess Texas Red−maleimide. Dye-conjugated virus was separated from the excess dye by sucrose gradient centrifugation.

**Fabrication of Patterned Capture Surfaces.** Capture surfaces containing single-stranded DNA complementary to the 5′ end of TMV genomic RNA were fabricated as previously described.[23] Briefly, gold patterns were fabricated onto silicon oxide wafers by photolithography and cut to produce individual chips (~6 mm × 25 mm) containing two electrically independent electrodes (1 mm × 8 mm, Figure 2). To deposit chitosan, chips were immersed in a 0.5% (w/v) chitosan solution, pH 3.7, and the left electrode negatively biased for 2 min at a constant current of 4 A/m$^2$. Chitosan deposited chips were then rinsed with DEPC-treated distilled water, neutralized in 1 N NaOH solution for 5 min, and equilibrated in 2×SSC buffer containing 0.1 M $MgCl_2$ (2×SSC+Mg). Electrodeposited chitosan was then activated by immersing in 0.05% (v/v) glutaraldehyde solution for 30 min with 75 rpm gyratory shaking. After thorough rinsing with the 2×SSC+Mg buffer, the chips were placed in a 2 mL microcentrifuge tube containing 2×SSC+Mg buffer (no DNA negative control) or with 37 $\mu$g/mL terminal amine group functionalized probe DNA for either the TMV 5′ end (GTTTGTTGTTGTTGGTAATTGTTG-$NH_2$) or a hexahistidine coding sequence ($H_2$N-ATGATGATGATGATGATG) at 4 °C overnight. Chips were then thoroughly rinsed with the 2×SSC+Mg buffer and reacted with dilute $NaBH_4$ solution for 5 min to reduce the Schiff base to a stable secondary amine linkage. Finally, the chips were immersed in a solution of salmon sperm DNA (1 mg/mL) for 1 h at room temperature to block nonspecific binding sites before hybridization.

**Spatially Selective Assembly of TMV Nanotemplates via Hybridization.** Silicon chips containing no DNA oligos, oligos complementary to the TMV 5′ end, or oligos complementary to a hexahistidine sequence were rinsed with 2×SSC buffer and placed in 2 mL microcentrifuge tubes filled with 1 mL of fluorescent labeled TMV templates. Tubes were placed in a rotary shaker and incubated overnight at 30 °C. Chips were then rinsed three times with fresh 2×SSC buffer and analyzed via fluorescence microscopy using a Leica MZ FLIII microscope with a 560/55 nm excitation and 645/75 emission filter set. Photomicrographs

were prepared using a digital camera (Spot 32, Diagnostic Instruments) and processed for printing with Adobe Photoshop (Grand Prairie, TX). Fluorescence intensities were then analyzed using an image analysis software (ImageJ, http://rsb.info.nih.gov/ij/). For the RNase assays, 50 $\mu$g of RNase A was added to the partially disassembled virus for 30 min before the addition of the probe chip or to probe chips already hybridized to labeled TMV1cys. To visualize the chip surfaces, hybridized chips were rinsed with water, dried, and sputter coated with 60/40 platinum/palladium alloy. Coated chips were then viewed using a Hitachi S.4700 FE-SEM (Pleasanton, CA).

TMV1cys accumulated to near wild-type levels in infected tissues, indicating that the insertion of a single cysteine residue in the N-terminus of the coat protein did not significantly alter the biological fitness of the virus (data not shown). As shown in Figure 1, the addition of this cysteine residue was designed to produce a spatially arrayed pattern of reactive thiol groups along the outer surface of the virus template. To assess the ability of TMV1cys to function as a template for the deposition of nanoparticles, metal cluster formation was performed via the in situ chemical reduction of metal precursor ions as previously described[14] (Supporting Information). Results indicated that the TMV1cys template effectively bound solid clusters of gold and platinum, demonstrating the usefulness of this virus as a nanoparticle template.

Selectivity for binding to the engineered N-terminal cysteine residue was further investigated using thiol reactive maleimide-linked fluorescent dyes. Native TMV coat protein contains a cysteine residue at amino acid position 27; however, this residue is embedded within the central interior of the virion and should not be accessible for labeling.[5] Labeling experiments using either the wild-type or TMV1cys virus confirmed that only the engineered N-terminal cysteine group was accessible for labeling (Figure 3). Combined these findings demonstrate that TMV1cys provides a highly selective template for the attachment of thiol reactive molecules.

Molecular patterning represents a considerable obstacle in the fabrication of nanoscale devices. One proven method for the patterning of biomolecules has been through nucleic acid hybridization.[30,31] As outlined in Figure 2, we have taken advantage of TMV's natural ability to partially disassemble to direct its assembly onto a patterned device using a chitosan-based nucleic acid hybridization scheme. Specifically, readily addressable capture sites were generated by electrodepositing chitosan onto gold-patterned silicon oxide chips. Single-stranded probe DNAs, with or without specificity for the TMV 5′end RNA, were covalently conjugated onto the glutaraldehyde-activated chitosan layer to produce targeted assembly sites for fluorescent marker linked TMV1cys templates. As shown in Figure 4, only the patterned electrode linked to the TMV-specific probe bound the labeled TMV virions. Importantly, bare gold electrodes, silicon oxide surfaces, or chitosan-coated electrodes containing no DNA or noncomplementary DNA probes (hexahistidine sequence) did not yield any significant fluorescence, confirming that

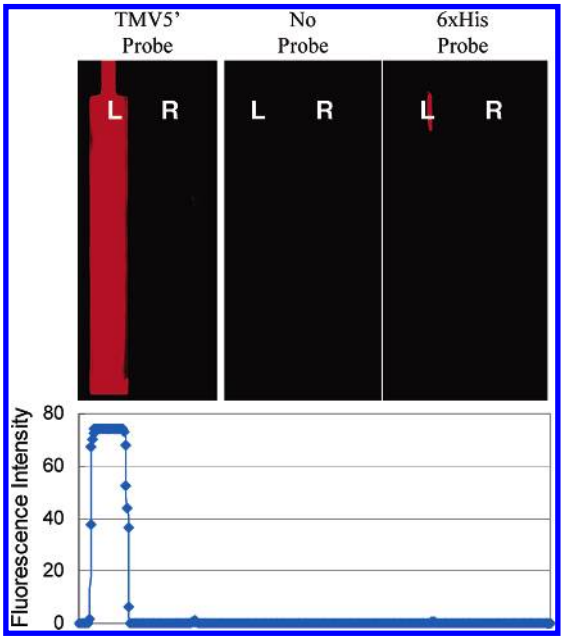


**Figure 4.** Patterned assembly of Texas Red labeled TMV1cys virions onto a capture surface via sequence-specific hybridization. Each chip contains a left (L) and right (R) electrode. Chitosan is electrodeposited only on the left electrode of each chip. The right electrode, as well as the silicon oxide area, on each chip carries no chitosan and functions as internal controls for nonspecific binding. Chips were immersed overnight in a 20 $\mu$g/mL solution of Texas Red-labeled TMV1cys and rinsed 3 $\times$ 5 min prior to examination by fluorescence microscopy. TMV5′ probe DNA complementary to the 5′ end genome sequence of TMV; no probe contains chitosan only; and 6$\times$His contains probe DNA complementary to six histidine codons. The graph under the fluorescence images shows fluorescence intensity profile anaysis.

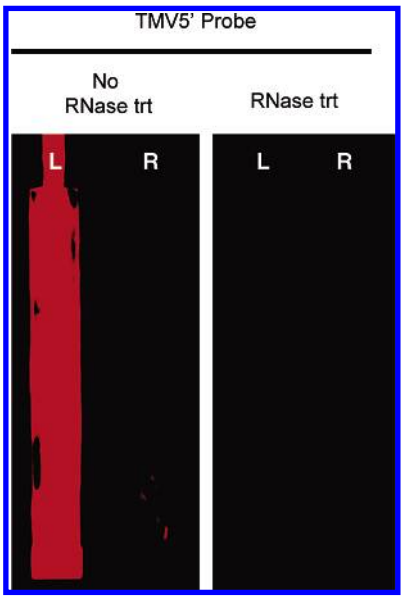


**Figure 5.** Hybridization of Texas Red labeled TMV1cys virions onto TMV specific probe chips with or without prior RNAse A treatment.

our hybridization-based TMV assembly scheme was sequence specific with minimal nonspecific interactions between viral templates and other exposed surfaces. The fluorescence intensity analysis (Figure 4) further confirmed

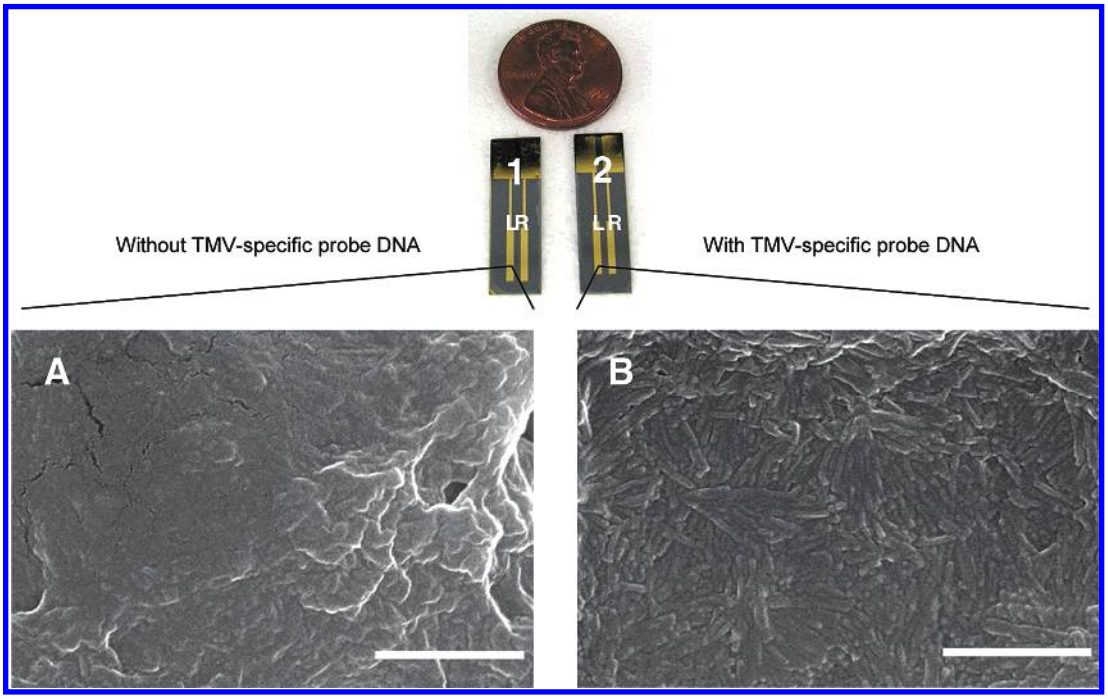


**Figure 6.** FE-SEM images of the assembled TMV1cys nanotemplates onto the capture surfaces with or without 5′-end complementary probe DNA. Panel A shows a chitosan layer without TMV specific probe DNA. Note that no virus-specific binding is observed. Panel B shows chitosan layer with TMV specific probe DNA. The virus can be seen densely packed across the surface of the electrode much like the pile of a carpet. This observation is consistent with the 5′ end of the virus rod being tethered to the gold support. Bar represents 500 nm.

negligible nonspecific binding, as well as high spatial selectivity of the TMV1cys assembly.

To further assess the requirement for hybridization in the patterning of labeled TMV1cys onto the probe electrodes, we incubated the partially disassembled virions in the presence of RNAse A before adding the chitosan chips (Figure 5). Exposure to RNAse would cleave the exposed single-stranded RNA sequences from the TMV virion and prevent probe hybridization but does not result in the further disassembly of the virus (data not shown). Results displayed in Figure 5 clearly show that RNAse A treatment prevented the binding of labeled virus onto the probe electrode, confirming the requirement of exposed RNA sequences for the patterned assembly of the virus templates.

We then further examined silicon chip surfaces via scanning electron microscopy (SEM) to confirm the orientation and patterned assembly of the virus templates. As shown in Figure 6, SEM revealed the presence of rod-shaped virions assembled along the length of electrodes coated with TMV 5′ end specific probe DNA. Virus templates were layered in a dense carpet-like fashion consistent with the virions being attached by one end to the electrode surface. In contrast, chitosan electrodes containing no probe DNA or incubated with RNAse A treated TMV1cys virions displayed no significant levels of bound virus (Figure 6, data not shown). These data clearly support the fluorescence data and demonstrate that only chip electrodes containing probe DNA specific to the TMV 5′ end were capable of patterning the labeled TMV1cys virions. The carpet-like appearance of these virions as well as the inability of RNase treated virus to assemble on the electrodes indicates that these templates are attached via the exposed 5′ end of the viral RNA. Furthermore, hybridized viral templates remained attached to the chip through vigorous rinsing, air-drying, extended storage, and/or metal coatings. This stability suggests that this hybridization-based assembly strategy represents a robust platform for the patterning of nanotemplates.

To further explore the stability of the attached TMV1cys templates, probe chips hybridized with the fluorescently labeled TMV1cys templates were incubated overnight with 50 $\mu$g of RNase A. Micrographs taken before and after RNase A treatment show only a limited loss of fluorescence along the edges of the probe electrode (Figure 7), indicating a significant stability of the assembled virions against the RNase A treatment. It seems likely that the densely packed and oriented virus templates function to inhibit access to the exposed 5′ end RNA. This stability further suggests that this hybridization-based assembly strategy provides a robust platform for the patterning of these nanotemplates.

In this study we have utilized several strategies to enhance the use of TMV as template for both the production and patterned assembly of nanoscale materials. First, the development of a genetically engineered TMV template provided a simple and direct means for the coupling of both inorganic and organic compounds to the virus surface. This was accomplished by inserting a cysteine residue onto the outer surface of the virus coat protein, providing an accessible thiol group that could be easily targeted as a covalent attachment site using standard conjugation chemistries. Second, we took advantage of the TMV evolutionary adaptation that permits removal of a few coat protein subunits from the 5′ end of the viral RNA. Removal of these subunits via a simple

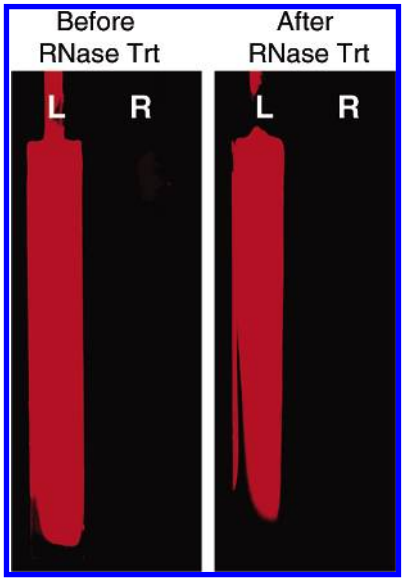


**Figure 7.** RNase A treatment of an entire probe chip prehybridized with Texas Red labeled TMV1cys virions. Micrographs show the same chip before and after an overnight incubation with RNase A.

centrifugation step allowed functionalized virus templates to be specifically addressed through nucleic acid hybridization. Finally, we utilized chitosan as an interface to direct the spatially selective assembly of the viral templates onto the surface of a gold-patterned silicon chip by applying electrical signal. Combined, these strategies provide the bases for further efforts to utilize viral templates in the construction of nanodevices.

**Acknowledgment.** We wish to thank Tim Maugel in the Laboratory for Biological Ultrastructure for assistance with FE-SEM viewing. This work was supported in part by DOE award DE-FG02-02ER45975 & 76 and the Laboratory for Physical Sciences.

**Supporting Information Available:** Deposition of metal cluster onto TMV1cys templates. This material is available free of charge via the Internet at http://pubs.acs.org.

## References

(1) Braun, E.; Eichen, Y.; Sivan, U.; Ben-Yoseph, G. *Nature* **1998**, *391*, 775−778.
(2) Keren, K.; Berman, R. S.; Buchstab, E.; Sivan, U.; Braun, E. *Science* **2003**, *302*, 1380−1382.
(3) Douglas, T.; Young, M. *Nature* **1998**, *393*, 152−155.
(4) Mao, C. B.; Flynn, C. E.; Hayhurst, A.; Sweeney, R.; Qi, J. F.; Georgiou, G.; Iverson, B.; Belcher, A. M. *Proc. Natl. Acad. Sci. U.S.A.* **2003**, *100*, 6946−6951.
(5) Namba, K.; Pattanayek, R.; Stubbs, G. *J. Mol. Biol.* **1989**, *208*, 307−325.
(6) Dawson, W. O.; Beck, D. L.; Knorr, D. A.; Grantham, G. L. *Proc. Natl. Acad. Sci. U.S.A.* **1986**, *83*, 1832−1836.
(7) Dujardin, E.; Peet, C.; Stubbs, G.; Culver, J. N.; Mann, S. *Nano Lett.* **2003**, *3*, 413−417.
(8) Shenton, W.; Douglas, T.; Young, M.; Stubbs, G.; Mann, S. *Adv. Mater.* **1999**, *11*, 253−256.
(9) Fowler, C. E.; Shenton, W.; Stubbs, G.; Mann, S. *Adv. Mater.* **2001**, *13*, 1266−1269.
(10) Knez, M.; Bittner, A. M.; Boes, F.; Wege, C.; Jeske, H.; Maiss, E.; Kern, K. *Nano Lett.* **2003**, *3*, 1079−1082.
(11) Knez, M.; Sumser, M.; Bittner, A. M.; Wege, C.; Jeske, H.; Martin, T. P.; Kern, K. *Adv. Funct. Mater.* **2004**, *14*, 116−124.
(12) Schlick, T. L.; Ding, Z. B.; Kovacs, E. W.; Francis, M. B. *J. Am. Chem. Soc.* **2005**, *127*, 3718−3723.
(13) Mao, C. B.; Solis, D. J.; Reiss, B. D.; Kottmann, S. T.; Sweeney, R. Y.; Hayhurst, A.; Georgiou, G.; Iverson, B.; Belcher, A. M. *Science* **2004**, *303*, 213-217.
(14) Lee, S. Y.; Royston, E.; Culver, J. N.; Harris, M. T. *Nanotechnology* **2005**, *16*, s435-s441.
(15) Steckert, J. J.; Schuster, T. M. *Nature* **1982**, *299*, 32−36.
(16) Lomonossoff, G. P.; Butler, P. J. G. *FEBS Lett.* **1980**, *113*, 271−274.
(17) Wilson, T. M. A.; McNicol, J. W. *Arch. Virol.* **1995**, *140*, 1677−1685.
(18) Wilson, T. M. A. *Virology* **1984**, *137*, 255−265.
(19) Piner, R. D.; Zhu, J.; Xu, F.; Hong, S. H.; Mirkin, C. A. *Science* **1999**, *283*, 661−663.
(20) Odom, T. W.; Love, J. C.; Wolfe, D. B.; Paul, K. E.; Whitesides, G. M. *Langmuir* **2002**, *18*, 5314−5320.
(21) Pathak, S.; Dentinger, P. M. *Langmuir* **2003**, *19*, 1948−1950.
(22) Kane, R. S.; Takayama, S.; Ostuni, E.; Ingber, D. E.; Whitesides, G. M. *Biomaterials* **1999**, *20*, 2363−2376.
(23) Yi, H. M.; Wu, L. Q.; Ghodssi, R.; Rubloff, G. W.; Payne, G. F.; Bentley, W. E. *Anal. Chem.* **2004**, *76*, 365−372.
(24) Yi, H. M.; Wu, L. Q.; Ghodssi, R.; Rubloff, G. W.; Payne, G. F.; Bentley, W. E. *Langmuir* **2005**, *21*, 2104−2107.
(25) Wu, L. Q.; Gadre, A. P.; Yi, H. M.; Kastantin, M. J.; Rubloff, G. W.; Bentley, W. E.; Payne, G. F.; Ghodssi, R. *Langmuir* **2002**, *18*, 8620−8625.
(26) Turpen, T. H.; Reinl, S. J.; Charoenvit, Y.; Hoffman, S. L.; Fallarme, V.; Grill, L. K. *Bio/Technology* **1995**, *13*, 53−57.
(27) Higuchi, R.; Krummel, B.; Saiki, R. K. *Nucleic Acids Res.* **1988**, *16*, 7351−7367.
(28) Gooding, G. V.; Hebert, T. T. *Phytopathology* **1967**, *57*, 1285.
(29) Cheung, C. L.; Camarero, J. A.; Woods, B. W.; Lin, T. W.; Johnson, J. E.; De Yoreo, J. J. *J. Am. Chem.* Soc. **2003**, *125*, 6848−6849.
(30) Niemeyer, C. M. *Science* **2002**, *297*, 62−63.
(31) Keren, K.; Krueger, M.; Gilad, R.; Ben-Yoseph, G.; Sivan, U.; Braun, E. *Science* **2002**, *297*, 72−75.

NL051254R